GeoAmericas2020
4th PAN AMERICAN CONFERENCE ON GEOSYNTHETICS
26-29 APRIL 2020 • RIO DE JANEIRO • BRAZIL

Nonlinearity of stress and strain in reinforced homogenized two-layered triaxial specimens

G. M. Oliveira, Department of Civil Engineering and Architecture, University of Beira Interior, Covilhã, Portugal
I. M. C. F. G. Falorca, Department of Civil Engineering and Architecture, University of Beira Interior, Covilhã, Portugal
L. J. Andrade Pais, Department of Civil Engineering and Architecture, University of Beira Interior, Covilhã, Portugal.

ABSTRACT
The stress–strain relationship of a homogeneous specimen in triaxial compression test allow to estimate a suitable understanding of stiffness parameters. However, when a two-layered specimen is tested the characterization of the stress–strain behavior for two-layered soil is mainly complex due to the nonlinearity of the deformations. A homogenization approach was adopted to determine the initial Young's modulus of the supposed cross-anisotropic linear elastic medium. Triaxial compression tests were carried out on both homogeneous and two-layered specimens under a low effective confining pressure of 30 kPa. A model 3D printed geogrid was fabricated to fit in the interaction between aggregate and sand–rubber mixture. The nonlinear stress–strain relationship for unreinforced and reinforced homogenized two-layered triaxial specimens was formulated by a well-known hyperbolic model which involves Mohr-Coulomb strength parameters. The initial Young's modulus for the cross-anisotropic medium was used in the hyperbolic model to characterize the stress–strain behavior of unreinforced and 3D printed geogrid reinforced soils specimens. In this study was proposed analysis of a well-known nonlinear model involving effect of unreinforced and reinforced homogenized two-layered specimen.

1. INTRODUCTION

In soil mechanics the triaxial test is extensively applied in engineering practice and research to investigate the stress–strain relationship of homogeneous specimens of undisturbed and remolded soils. The Mohr-Coulomb parameters are used by geotechnical engineering software in order to quantity the soil strength. Natural or artificial layered soils are not commonly studied due to the complexity in measuring strains. The first investigation of detailed strains in layered soils performed in drained triaxial compression test was observed by Arthur and Phillips (1975). This study showed that the stress–dilatancy relationship for the maximum stress ratio supported by homogeneous samples in triaxial test was linear and independent of inherent anisotropy and porosity. This relationship was used to predict maximum stress ratios in layered and reinforced samples. Furthermore, the author also concluded that the loose material in a layered soil dilated at a rate much higher than reached in drained tests on homogeneous loose samples of the same porosity and much closer to that reached in homogeneous dense samples.

The objective of the article is adapting the Duncan and Chang (1970) hyperbolic model with the use of the equivalent or homogenized elastic modulus in vertical direction which is lower than horizontal direction in cross-anisotropic medium, in order to characterize the stress–strain behavior of the two-layered specimens with and without model 3D printed geogrid. To accomplish this, was used the raw force–displacement data as well as the experimental stress–strain relationships of homogeneous specimens to develop better understanding of interfaces involving soil–geogrid.

Duncan and Chang (1970) established a simplified nonlinear stress–strain relationship for soils. The nonlinearity of the stress–strain relationship for soil may be approximated by hyperbole as reported by Kondner (1965). According to the Duncan and Chang (1970) the hyperbolic equation proposed by Kondner was an important part of the nonlinearity of the soil stress–strain behavior. The stress–dependency depending on the initial tangent modulus which have a relationship with confining pressure, except in the case of unconsolidated–undrained (UU) tests, was proposed by Janbu (1963). Duncan et al. (1980) complied hyperbolic parameters for about 150 different soils, the report was concerned with the use of values of Young's modulus and bulk modulus to represent the nonlinear and stress dependent stress–strain and volume change behavior of soils.

In the geotechnical field which involve rock or soil masses consisting of numerous strata on which many loads (normal, shear or rotational) are applied, in any analysis it would be an extremely complex operation to take into count the individual properties of each of these strata. However, under certain conditions the system of strata can be replaced by an "equivalent" homogeneous cross-anisotropic material (Salamon 1968). In soil mechanics, the cross-anisotropic was

approached in some studies as (Atkinson 1975, Gazetas 1981, Gibson 1974, Poulos and Davis 1974). Guo and Stolle (2017) proposed a homogenization approach to determine the "equivalent" elastic properties for a layered medium, with each layer being a linear elastic isotropic material. The authors demonstrated that stress (or strain) path under K_o compression, plane strain compression and compression under hydrostatic pressure are sufficient to determine five independent elastic constants of cross-anisotropic (or transversely isotropic) soil.

3D printing has been used in several investigations such as (Hanaor et al., 2016), (Miskin and Jaeger, 2013), (Stathas, Wang and Ling, 2017), (Viswanadham and König, 2004). For instance, Hanaor et al. (2016) proposed three approaches for the 3D generation of model grains, triaxial tests have been performed on 3D-printed particles in order to results of these tests show the ability of the printed particles to reproduce soil behavior and demonstrate the effect of particle shape on the material response. Miskin and Jaeger (2013) verified with 3D printing the results of particles that produce aggregate which has become stiffen under compression. Stathas, Wang and Ling (2017) fabricated small model geogrids with the aim of scaling the model geometry and tensile behavior up to 5% strain. In the research also was fabricated models with tensile strength close to one-tenth of prototypes, which is desirable for 1:10 model tests under 10-g condition in centrifuges. Viswanadham and König (2004) provided a set of guidelines for selecting a model geogrid for physical model studies, especially in a geotechnical centrifuge, for which was performed simple dimensional analysis, the relevant scale factors for modeling of geosynthetic materials for both 1-g and N-g tests.

2. BACKGROUND

The principles of homogenization of two-layered soil are the basis of this study to evaluate the stress–strain behavior. The elastic modulus for the cross-anisotropic material was used in the hyperbolic model to understating the stress–strain behavior of the two-layered specimens. Here, and in the rest of this study each layer has separately a linear elastic behavior. Salamon (1968) said that all layers are homogeneous, cross-anisotropic and that their thickness and elastic properties vary randomly with the depth below surface. Moreover, the rock mass remains continuous after deformation and no relative displacement takes place at the interfaces between the layers. In Skrzypek and Ganczarski (2015), they represented the matrix form which the stress–strain relationship can be expressed for transversely isotropic (or cross-anisotropic) linear elastic behavior, when the z-axis is perpendicular to the bedding planes as

$$\begin{Bmatrix} \varepsilon_{xx} \\ \varepsilon_{yy} \\ \varepsilon_{zz} \\ \gamma_{xy} \\ \gamma_{yz} \\ \gamma_{zx} \end{Bmatrix} = \begin{pmatrix} 1/E_h & -\upsilon_{hv}/E_h & -\upsilon_{vh}/E_v & & & \\ -\upsilon_{hh}/E_h & 1/E_h & -\upsilon_{hh}/E_v & & & \\ -\upsilon_{hv}/E_h & -\upsilon_{hv}/E_h & 1/E_v & & & \\ & & & 1/G_{hh} & & \\ & & & & 1/G_{hv} & \\ & & & & & 1/G_{vh} \end{pmatrix} \begin{pmatrix} \sigma_{xx} \\ \sigma_{yy} \\ \sigma_{zz} \\ \tau_{xy} \\ \tau_{yz} \\ \tau_{zx} \end{pmatrix} \quad [1]$$

where E_h and E_v are the elastic moduli in the horizontal and vertical directions, respectively. υ_{vh} is the Poisson's ratio for effect of vertical strain on horizontal strain and υ_{hv} is the Poisson's ratio for effect of horizontal strain on vertical strain. υ_{hh} is the principal Poisson's ration of strain in the horizontal direction caused by strain in the horizontal direction. G_{hh}, G_{hv} and G_{vh} are shear moduli in each plane, τ is the shear stress, γ is the shear strain, ε is the normal strain and σ is normal stress. The symmetry in the matrix produces the important result that the G_{hh} is not independent which implies that the five elastic constant (E_h, E_v, υ_{vh}, υ_{hh} and υ_{hv}) are inter-related by:

$$G_{hh} = \frac{nE_v}{2(1+\upsilon_{hh})} \quad [2]$$

with

$$n = \frac{\upsilon_{hv}}{\upsilon_{vh}} = \frac{E_h}{E_v}$$

Isotropy is the special case of anisotropy with $\upsilon_{vh} = \upsilon_{hh} = \upsilon_{hv} = \upsilon$ and n = 1. However, limitations are placed on the values of the elastic constants which strain energy function must be positive as (e.g. Barden 1963).

$$1 > \upsilon_{hh}^2 + 2\upsilon_{hv}\upsilon_{vh} + 2\upsilon_{hh}\upsilon_{hv}\upsilon_{vh}$$

$$1 > \upsilon_{hh} + 2\upsilon_{hv}\upsilon_{vh}$$

The homogenization approach was used to determine the elastic properties of layered soil, in the special case with two constituent materials (Guo and Stole 2017). The authors correlated equivalent elastic properties of a multi-layered medium

containing two constituent materials, where φ_1 and φ_2 were the normalized thickness (or volume fraction). The elastic properties of layered medium with two constituent materials can be related to Eq.1 as

$$\upsilon_{hh} = \frac{\frac{E_1}{E_2}\varphi_1\upsilon_1(1-\upsilon_1^2) + \varphi_2\upsilon_2(1-\upsilon_1^2)}{\frac{E_1}{E_2}\varphi_1(1-\upsilon_1^2) + \varphi_2(1-\upsilon_1^2)} \quad [3]$$

$$\upsilon_{hv} = (1-\upsilon_{hh})\left(\frac{\varphi_1\upsilon_1}{1-\upsilon_1} + \frac{\varphi_2\upsilon_2}{1-\upsilon_2}\right) \quad [4]$$

$$E_h = (1-\upsilon_{hh}^2)\left(\frac{E_1\upsilon_1}{1-\upsilon_1^2} + \frac{E_2\upsilon_2}{1-\upsilon_2^2}\right) \quad [5]$$

$$\frac{1}{E_v} = \frac{\varphi_1}{E_1}\left(1 - \frac{2\upsilon_1^2}{1-\upsilon_1}\right) + \frac{\varphi_2}{E_2}\left(1 - \frac{2\upsilon_2^2}{1-\upsilon_2}\right) + \frac{2\upsilon_{hv}^2}{(1-\upsilon_{hh})E_h} \quad [6]$$

$$\frac{1}{G_{hv}} = \frac{1}{2}\left[\frac{\varphi_1}{E_1}(1+\upsilon_1) + \frac{1}{E_2}\varphi_2(1+\upsilon_2)\right] \quad [7]$$

3. MATERIALS

3.1 Aggregate and sand–rubber mixture

Figure 1 shows the grain-size distribution curves of three materials that were used in the specimen preparation. The stone aggregate is a 100% crushed granite supplied by a quarry in the region (Meimoa quarry), which is mapped as a medium- to coarse-grained two-mica granite, with a specific gravity of 2.63. The stone aggregate was sieved to get the required 8-15mm size fraction, classified as GP - poorly graded gravel, according to the Unified Soil Classification System (ASTM D2487). This aggregate was reused several times, after being re-sieved on each test. The good hardness of the granite aggregate minimized the amount of particle crushing experienced during shear. The sand, made of quartz, consists of particles with a specific gravity of 2.65. The rubber aggregate, resulting from the grinding of used tires, consists of particles with a specific gravity of 1.16. The sand–rubber (S–R) mixture particles was prepared by arrangement in thin layers in order to avoid segregation of the components and to obtain a homogeneous material and a weak soil. Based on the study carried out by Kim and Santamarina (2008), a 55% rubber particle fraction and 33% porosity, defined by the ratio of the rubber volume to the total solids volume, was adopted, resulting in a volume of sand sufficient for fill the voids between the rubber particles. The unpaved roads reinforced with geogrid are built on soft soils occurring in subgrade with a CBR of less than 3% (Giroud and Han, 2004). The Figure 2 (a), b)) shows a CBR test carried out in the homogeneous layer of (S–R) mixture which presented a CBR value of 2%. The mixture was used as a weak soil in the triaxial test and the same particle fraction was performed afterward.

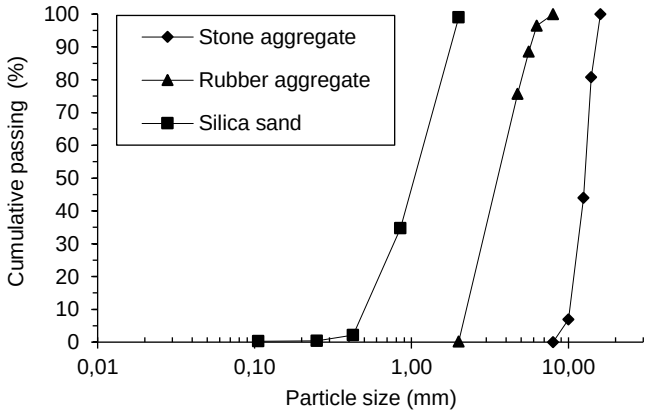

Figure 1. Grain-size distribution curves for test materials.

a) Test apparatus for application of forces

b) Test specimen after the test

Figure 2. CBR test.

3.2 3D printed geogrid

The geogrid was fabricated by 3D printing, using the printer Objet 500 Connex 3. The technology used to print the model geogrids was Stereolithography (SLA) to the digital material used to print it were Veroblackplus and TangoPlus - RGD 8560, which admit sufficiently rigid in scaled experiments with 1-g (Stathas et al., 2017). The Table 1 shows the RGD 8560 properties used in this paper. The geogrids were designed in CAD software, such as software Rhinoceros, reproducing the geometry on a scale of 1:3 from a commercial geogrid. The printed geogrids were designed with different shapes it was due to the two different tests performed, triaxial compression test (circular shape) and tensile test (square shape with dimensions of 10x10 cm) (see, Figure 3a). The printing direction has significant effects on the stiffness and tensile strength of the geogrid, a 45º direction was adopted to obtain a uniform 3D printing. In this study the characteristics of the biaxial geogrid were equally designed in longitudinal and transversal directions as is shown in Figure 3b.

Table 1. Mechanical properties of RGD 8560 (Digital Material).

Mechanical properties	Test Method	RGD 8560-DM
Tensile strength (MPa)	ASTM D638	29-38
Modulus of elasticity (MPa)	ASTM D638	1100-1700
Elongation strain at break (%)	ASTM D638	25-35
Density (g/cm³)	ASTM D1505	0.9

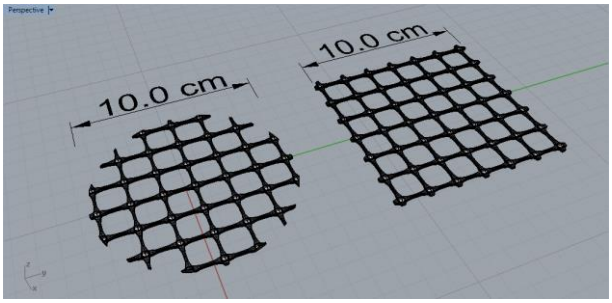

a) Circular and square shape

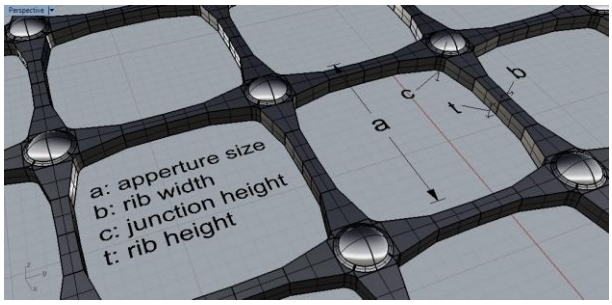

b) Equal characteristics of the printed biaxial geogrid

Figure 3. Geogrids designed in CAD software.

4. PROGRAMME OF TESTING

4.1. Tensile test

The tensile properties of the geogrid were determined from the results of a tensile test performed according to the method described in standard ASTM D4595. All the specimens, with a nominal width of 100 mm, were attached to the grippers of the tensile equipment to ensure a nominal length of 50 mm. The equipment was adjusted to operate at a constant tensile speed of 1.0 mm/min. Although these tests were carried out according to the standard procedure, an adjustment to the rate of extension was made in order to simulate the deformation rate of geodrid during the triaxial test. Figure 4 shows the evolution of the tensile force with increasing the actual length of the specimens during the test.

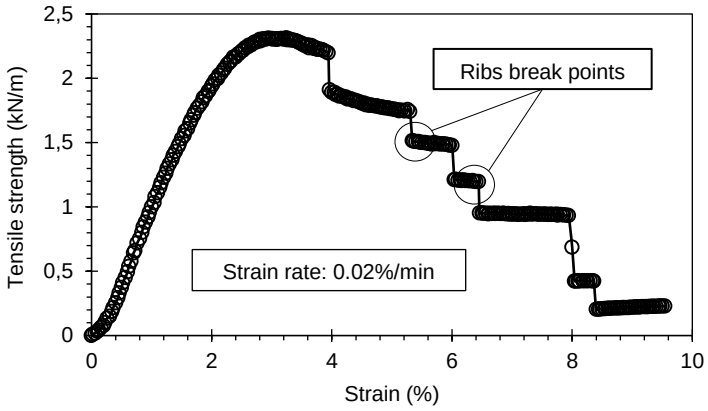

Figure 4. Tensile Test performed on geogrid 3D printed.

4.2. Triaxial Test

In this study the apparatus used to perform triaxial compression tests in two-layered cohesionless soil followed ASTM standard (ASTM D4767). The tests required for the characterization of the materials related to item 3.1 and 3.2, triaxial compression tests were performed by loading the specimens at a constant rate of deformation. Although pressure control was available in the triaxial cell, it was decided to impose the desired confining pressure by applying suction at the base of the specimen by means of a vacuum, as a backpressure, which made it possible to simplify considerably execution of the test. Each specimen was tested under controlled deformation conditions, imposing the constant axial deformation rate of 1 mm/min, until an axial extension of 20% was achieved. This extension was evaluated, at each instant, from the relative external displacement and assuming the simplifying hypothesis of uniform distribution of the axial deformation in the specimen. The Figure 5 represents the triaxial two-layered specimen before and after to be performed.

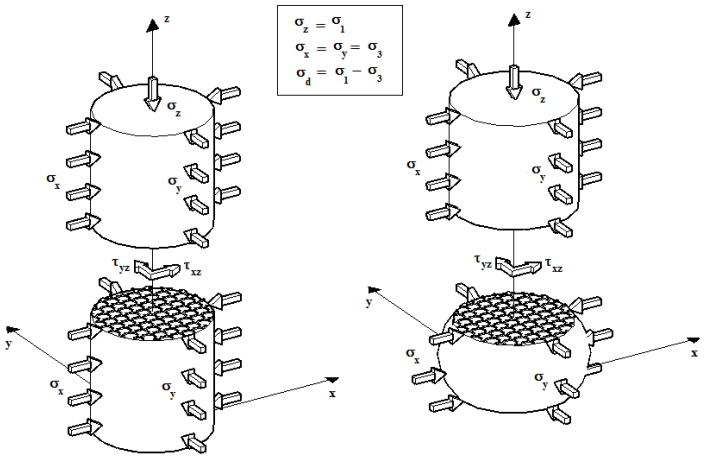

Figure 5. Schematic representation of the two-layered specimen performed on triaxial test with 3D printed geogrid at the interface.

The specimen preparation concerned with its errors associated such as leakage, tilting and seating, alignment and frictional ends. The rubber membrane was chosen to avoid pinholes and consequently leakage. The end of the aggregate layer was levelled in order to avoid tilting and seating errors at the top cap. The mold was attached to the pedestal to maintain the alignment of the sample. Although there is no water in the test, the filter paper was placed on the top and base of the pedestal to avoid sand grains coming out. The specimen (100 mm diameter and 200 mm height, to minimize dimensional effects) was previously jacketed with a rubber membrane (with vacuum) and placed on the triaxial cell pedestal. The procedure consisted of:

- place the mixture of rubber and sand in the lower half of the mold, as described in item 3.1. The unit weight was 12.03 kN/m³, estimated from mass weights of the volumetric fractions of the components (e.g. Kim and Santamarina 2008), corresponding to an initial void ratio of 0.49;
- place the 3D printed geogrid (when applicable);
- place the aggregate in the upper half of the mold in 5 equal layers. The value of the unit weight was 14.36 kN/m³, evaluated from the apparent volume and the mass of the aggregate, with an initial void ratio of 0.80;
- place the top plate and remove the mold by applying a vacuum inside the specimen, enough to maintain its geometry;
- place the o-rings in the specimen and confine it with deaired water, set the water confining pressure (10kPa) and vacuum confining pressure (20kPa).

5. RESULTS AND DISCUSSION

The elastic properties of layered soil are shown in Table 2, which the parameters of Eq. 3 to Eq. 7 can be determined, where the normalized thickness for both soils are 0.5 ($\varphi_1 = \varphi_2 = 0.5$), aggregate Young's modulus (E_1) is 15880 kPa, sand-rubber mixture Young's modulus (E_2) is 3013 kPa, aggregate Poisson's ratio (υ_1) is 0.23 and sand-rubber mixture Poisson's ratio (υ_2) is 0.45. In this study the elastic moduli in the vertical direction (E_v) of the two-layered specimen was considered in the proposed model as the initial tangent modulus (Ei), which replaces Janbu's formulation in comparison with the well-known hyperbolic model. Furthermore, the requirement for positive strain energy satisfy the constraints imposed for a cross-anisotropic material.

Table 2. Model parameters for reference cross-anisotropic medium

E_h (kPa)	E_v (kPa)*	υ_{hh}	υ_{hv}	G_{hh} (kPa)
9521	8424	0.27	0.41	7158

* Homogenized equivalent stiffness of two-layered specimen considered in the hyperbolic model proposed.

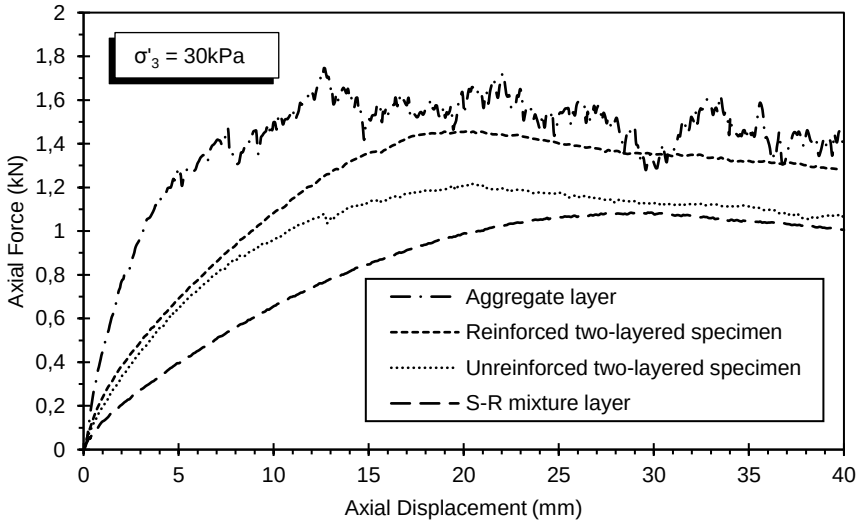

Figure 6. Axial force x axial displacement (raw data).

Figure 6 shows the force–displacement relationship for the different types of specimens. The raw data was not correlated directly with stress–strain relationship of the two-layered specimen, because the inherent anisotropic of the two-layered affects the strain prediction. In this study the average area of reinforced and unreinforced samples had a different variation rate of homogeneous samples, where the weak soil had higher dilation when performed in two-layered sample than homogenous sample. The axial force was divided by the average area, for a drained triaxial compression test, which was obtained the deviator stress ($\sigma'_1 - \sigma'_3$) and hence the stress ratio (σ'_1 / σ'_3). Figure 7a illustrates the volume change during the test for all samples tested. The raw-data shows that the maximum force achieved by the samples (unreinforced and reinforced) was sustained by the highest volumetric variation rate which is around 18 mm of axial displacement. Figure 7b shows the close-up view up of Fig. 7a. The aggregate layer begins to dilate approximately 1.5 mm axial displacement, while the sand–rubber mixture layer starts to dilate around 7 mm axial displacement, even as the reinforced and unreinforced layers. The volume change behavior of the two-layered specimen (reinforced and unreinforced) is closer to the volume change behavior of the sand-rubber mixture layer than to aggregate layer.

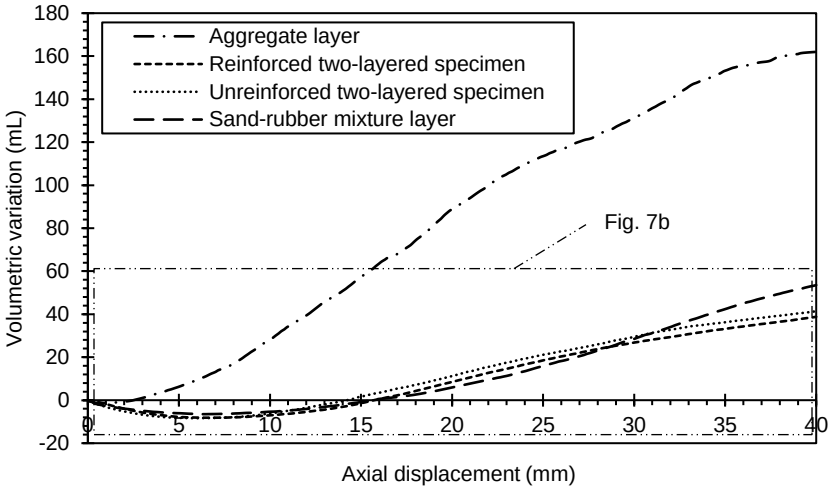

a) Overall axial force–displacement relationship.

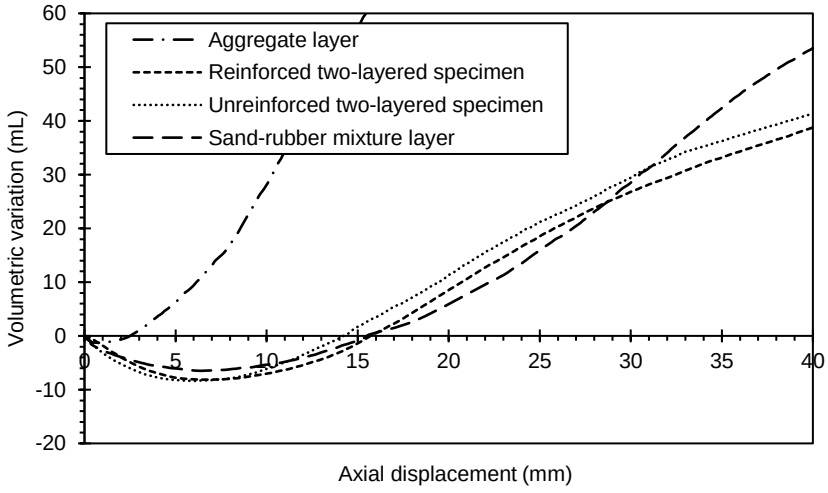

b) close-up view up of Fig. 7a.

Figure 7. Volumetric variation (mL) x axial displacement (mm) (raw data).

Figure 8 illustrates the stress–strain relationship estimation of the aggregate and S–R mixture with the well-known hyperbolic model, as well as the region of stress–strain behavior of the two-layered soils with Rf range from 0,7 to 0,9. The values of K and n for aggregate and S–R mixture were obtained with previous experiments with different confining pressures (15, 30 and 60 kPa), in agreement with the log–log graph proposed by Janbu (1963). For two-layered specimens

the homogenized equivalent stiffness was supported by the cross-anisotropic approach which consider that the elastic modulus in the vertical direction (Ev) was equal to the initial Young's modulus of the hyperbolic model (Ei). The homogenized equivalent stiffness corresponding to reinforced and unreinforced layer as a result of considering that there is no reinforcement action in deformations within the elastic limit. The upper- and lower-bound values of Rf were used with Mohr-Coulomb strength parameters c and ϕ, which can reasonably define the stress–strain behavior of two-layered soil. The drained angle of shearing resistance ϕ' used to aggregate, S–R mixture, reinforced and unreinforced specimens were determined as Arthur and Phillips (1975). In mixtures of soil and tire–rubber normally is observed an apparent cohesion (Rios et al. 2016, Masad et al. 1996). The triaxial test for different confining pressures were able to support the shear strength parameter for S–R mixture, which specifically presented the effective cohesion (c') at 20 kPa (see, Figure 9).

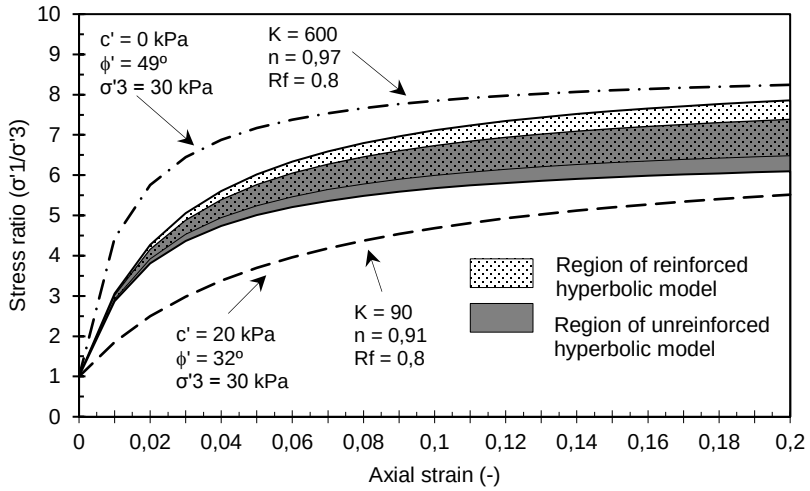

Figure 8. Calculated stress ratio (σ'_1/σ'_3) x axial strain.

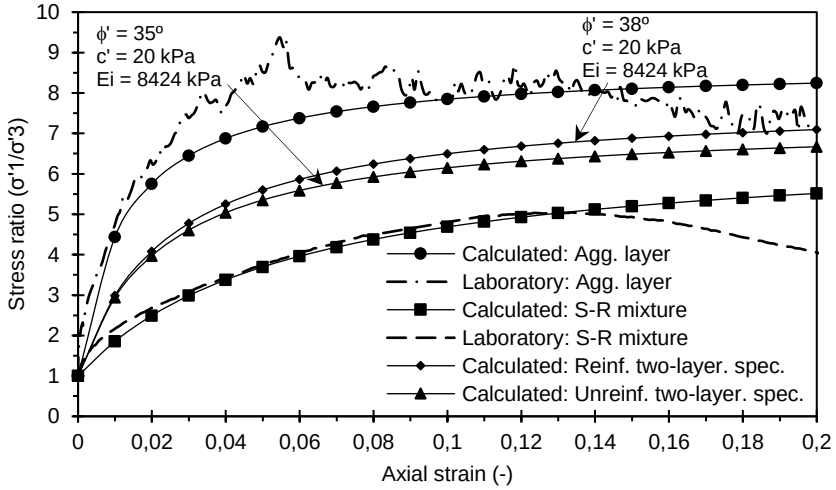

Figure 9. Laboratory and calculated stress ratio (σ'_1/σ'_3) x axial strain.

According to Balakrishnan and Viswanadham (2016) in order to maintain identical frictional bond area between model geogrid and the prototype geogrid, the percentage open area must be identical for ensuring perfect soil–geogrid interaction. In this study, the model geogrid characteristics were scaled-down of 1:3 from a commercial geogrid. Thus, the friction angle at soil–geogrid interface was identical with model and prototype. As shown in Figure 9 the addition of reinforcement to the layer increased the drained angle of shearing resistance by only 2 °. This effect may have been produced due to the tensile strength of the prototype at 2 and 5% of strain. The scale–down effect produced a model 3D printed geogrid not representative at 2% and 5% of strain. However, it should be considered that the strain rate of the tensile test of the model 3D geogrid was very low which as well as produces a lower tensile strength. The prototype which was simulated with geometry scale of 1:3 have an ultimate tensile strength of N^2 in comparison with the geogrid model, N is the scale factor

of the model in 1-g conditions. The selected 3D printed model geogrid should have $1/N^2$ times the tensile strength of the geogrid in the prototype as suggested in Viswanadham (2004).

6. CONCLUSIONS

Experimental results obtained from triaxial compression testing of homogeneous and two-layered specimens showed that the volumetric behavior as well as the stiffness and strength properties of the unreinforced and reinforced two-layered soil were closer to the weak soil or S–R mixture than the aggregate soil. The stress–strain behavior of two-layered soil until the failure can be approximated by a nonlinear elastic model associated with a cross-anisotropic approach. However, more tests with different materials at different scales must be performed in order to characterize the stress–strain behavior. Although this paper presented a prototype 3D printed geogrid with unrepresentative tensile strength at 2% and 5% of strain (less than 20 kN/m) in 1-g conditions, the purpose of this study was to investigate the layered soil with the cross-anisotropic approach associated with the hyperbolic model.

ACKNOWLEDGMENT

The lead author would like to gratefully acknowledge the scholarship BID/UBI - Santander Universidades/2018. This work is financed by Portuguese national funds through FCT – Foundation for Science and Technology, IP, within the research unit C-MADE, Centre of Materials and Building Technologies, University of Beira Interior, Portugal. This work is also supported with Portuguese national funds by FCT - Foundation for Science and Technology, I.P., within the GEOBIOTEC - UID/GEO/04035/2019.

REFERENCES

Arthur, J.R.F. and Philips, A.B. (1975). Homogeneous and layered sand in triaxial compression, *Géotechnique*, ICE Publishing, 25: 799-815.

ASTM D638, Standard Test Method for Tensile Properties of Plastics, *American Society for Testing and Materials*, West Conshohocken, Pennsylvania, USA.

ASTM D1505, Standard Test Method for Density of Plastics by the Density-Gradient Technique, *American Society for Testing and Materials*, West Conshohocken, Pennsylvania, USA.

ASTM D2487, Standard Practice for Classification of Soils for Engineering Purposes, *American Society for Testing and Materials*, West Conshohocken, Pennsylvania, USA.

ASTM D4595, Standard Test Method for Tensile Properties of Geotextiles by the Wide-Width Strip Method, *American Society for Testing and Materials*, West Conshohocken, Pennsylvania, USA.

ASTM D4767, Standard Test Method for Consolidated Undrained Triaxial Compression Test for Cohesive Soils, *American Society for Testing and Materials*, West Conshohocken, Pennsylvania, USA.

Atkinson, J. H. (1975). Anisotropic elastic deformations in laboratory tests on undisturbed London clay, *Géotechnique*, ICE Publishing, 25: 357-374.

Balakrishnan, S., Viswanadham, B.V.S. (2016). Performance evaluation of geogrid reinforced soil walls with marginal backfills through centrifuge model tests, *Geotextiles and Geomembranes*, Elsevier Ltd, 44: 95-108.

Barden, L. (1963). Stresses and displacements in a cross-anisotropic soil, *Géotechnique,* ICE Publishing, 13: 198-210.

Duncan, J.M. and Chang, C.Y. (1970). Nonlinear analysis of stress and strain in soil, *Journal of the Soil Mechanics and Foundations Division,* ASCE, 96: 1629-1653.

Duncan, J. M., Byrne, P., Wong, K. S. and Mabry, P. (1980). Strength, stress-strain, and bulk modulus parameters for finite element analyses of stresses and movements in soil masses, *Report No. UCB/GT/80-01*, University of California, College of Engineering, Berkeley, CA, USA.

Gazetas, G. (1981). Strip foundations on a cross-anisotropic soil layer subjected to dynamic loading, *Géotechnique*, ICE Publishing, 31: 161-179.

Gibson, R. E. (1974). The analytical method in soil mechanics, *Géotechnique*, ICE Publishing, 24: 115-140.

Giroud, J. P. and Han, J. (2004). Design method for geogrid-reinforced unpaved roads. II. Calibration and applications, *Journal of Geotechnical and Geoenvironmental Engineering*, ASCE,130: 787-797.

Guo, P. and Stolle, D.F.E. (2017). A physically meaningful homogenization approach to determine equivalent elastic properties of layered soil, *Canadian Geotechnical Journal*, NRC Research Press, 55: 303-311.

Hanaor, D. A. H., Gan, Y., Revay, M., Airey, D.W. and Einav, I. (2016). 3D printable geomaterials, *Géotechnique*, ICE Publishing, 66: 323-332

Janbu, N. (1963). Soil compressibility as determined by oedometer and triaxial tests, *European Conference on Soil Mechanics & Foundations Engineering*, Wiesbaden, Hessen, Germany, 1: 19-25.

Kim, H.K., and Santamarina, J.C. (2008). Sand–rubber mixtures (large rubber chips), *Canadian Geotechnical Journal*, NRC Research Press, 45: 1457-1466.

Kondner, R. L. and Horner, J. M. (1965). Triaxial compression of a cohesive soil with effective octahedral stress control, *Canadian Geotechnical Journal*, NRC Research Press, 2: 40-52.

Masad, E., Taha, R., Ho, C. and Papagiannakis, T. (1996). Engineering Properties of Tire/Soil Mixtures as a Lightweight Fill Material, *Geotechnical Testing Journal*, ASTM International, 19: 297-304.

Miskin, M. Z. and Jaeger, H. M. (2013). Adapting granular materials through artificial evolution, *Nature Materials*, Nature Publishing Group, 12: 326-331.

Poulos, H. G. and Davis, E. H. (1974). *Elastic solutions for soil and rock mechanics*, J. Wiley & Sons Inc., New York, NY, USA.

Rios, S., Fonseca, A. V., Kowalska, M. and Kijanka M. (2016). Misturas de Solo-Borracha para Isolamento de Vibrações. *In 15º Congresso Nacional de Geotecnia e 8º Congresso Luso-Brasileiro de Geotecnia*, Porto, Portugal. (in Portuguese).

Salamon M. D. G. (1968). Elastic moduli of a stratified rock mass. *International Journal of Rock Mechanics and Mining Sciences*, 5: 519-527.

Skrzypek, J.J. and Ganczarski, A.W. (2015). *Mechanics of anisotropic materials,* Springer, New York, NY, USA.

Stathas, D., Wang, J. P. and Ling, H. I. (2017). Model geogrids and 3D printing, *Geotextiles and Geomembranes*, Elsevier Ltd, 45: 688-696.

Viswanadham, B. V. S. and König, D. (2004). Studies on scaling and instrumentation of a geogrid, *Geotextiles and Geomembranes*, Elsevier Ltd, 22: 307-328.